Frontiers in Bioscience Landmark

Front. Biosci. (Landmark Ed) **2025**; 30(2): 25522
https://doi.org/10.31083/FBL25522

Original Research

Hypoxia-Induced *VGF* Promotes Cell Migration and Invasion in Prostate Cancer via the PI3K/Akt Axis

Leilei Wang[1,†], Ting Zhang[1,†], Yanning Qian[1], Yingying Wu[1], Ting Li[1], Yongbo Zheng[2], Chunli Luo[1], Xiaohou Wu[2], Tingmei Chen[1], Liping Ou[1,*]

[1]The Key Laboratory of Diagnostics Medicine designated by the Ministry of Education, Chongqing Medical University, 400016 Chongqing, China
[2]Department of Urology, The First Affiliated Hospital of Chongqing Medical University, 400016 Chongqing, China
*Correspondence: ouliping963@cqmu.edu.cn (Liping Ou)
[†]These authors contributed equally.

Academic Editor: Jordi Sastre-Serra
Submitted: 3 July 2024 Revised: 5 December 2024 Accepted: 13 December 2024 Published: 20 February 2025

Abstract

Background: Metastasis is a major cause of prostate cancer (PCa)-related deaths in men. Recent studies have indicated that VGF nerve growth factor inducible (VGF) affects tumor invasion and metastasis. The present study investigated whether VGF is abnormally expressed in PCa and affects PCa progression and investigated the specific regulatory mechanisms by which VGF affects PCa invasion and metastasis. **Methods**: The sh- hypoxia-inducible factor1 alpha (HIF-1α) plasmid was transfected into human cell lines 22Rv1 and C4-2 to create cell lines with stable low expression and overexpression of VGF. Quantitative PCR (qPCR) was performed to detect *VGF* mRNA. Western blot was performed to detect invasive migration-related proteins. Akt activator SC79 (4 µg/mL) was added. After adding docetaxel (4 nM) to cells transfected with sh-NC and sh-VGF, the capacity of the cells to migrate invasively was assessed using the Transwell and scratch assays. Nude mice were injected with cells stably transfected with sh-NC or sh-VGF and the metastasis of the cancer cells was detected by live imaging and HE staining after the injection of docetaxel (10 mg/kg). **Results**: Abnormal levels of VGF in PCa tissue and plasma samples were detected, and *VGF* knockdown suppressed PCa metastasis. VGF was also shown to affect the invasion and metastasis of PCa cells via PI3K/Akt signaling. *VGF* knockdown limited PCa metastasis and the inhibitory impact was higher when paired with docetaxel ($p < 0.001$). After hypoxia induction, both the mRNA and protein levels of *VGF* and HIF-1α increased, which is associated with a poor prognosis for PCa. **Conclusion**: By stimulating the PI3K/Akt pathway, VGF encourages the invasive metastasis of PCa. As a result, targeting *VGF* may be a potential treatment approach for metastatic PCa therapy.

Keywords: metastasis; PI3K/Akt; prostate cancer; *VGF*

1. Introduction

Prostate cancer (PCa) is one of the most common cancers worldwide [1]. According to the estimate by the American Cancer Society, the United States recorded over 268,000 new cases of PCa and 34,500 fatalities due to the disease in 2022 [2]. The vast majority of middle-aged and older adults will develop histological benign prostatic hyperplasia (BPH), a condition that is commonly associated with lower urinary tract symptoms (LUTS). BPH is a common diagnosis among the aging male population with increasing prevalence [3,4]. It is noteworthy that the high mortality and poor prognosis are associated with distant metastasis of PCa [5,6]. Currently, metastatic prostate cancer (mPCa) is primarily managed with androgen deprivation and chemotherapy [7,8]. Although the detection and treatment of this metastatic disease have advanced significantly [9], it remains largely incurable; the majority of patients remain resistant to long-term treatment, resulting in castration-resistant prostate cancer (CRPC) [10,11]. Therefore, there is an urgent need to find a novel therapeutic agent and biomarker for PCa clinical therapy in order to develop more effective treatments.

VGF was initially identified as a gene induced by nerve growth factor in the rat pheochromocytoma cell line PC12. *VGF* is extensively expressed in neuronal and neuroendocrine cells [12,13]. VGF nerve growth factor inducible (VGF) is a member of the secretogranin/chromogranin family of proteins, which can be upregulated by a variety of neurotrophic factors, including brain-derived neurotrophic factor (BDNF), 5-hydroxytryptamine (5-HT), and neurotrophin-3 (NT-3) [14,15]. In cancer, high expression of VGF is associated with advanced tumor stage, as well as perineural remodeling and perineural invasion in patients with pancreatic ductal adenocarcinoma [16,17]. Several studies have also revealed a role for VGF in squamous cell carcinoma, which is significantly associated with maintaining the squamous cell carcinoma phenotype [18,19]. Moreover, VGF positively correlates with radioresistance in PCa [20]. Although these studies suggest that VGF is upregulated in cancer, they have not investigated the functional role of VGF in PCa progression.

Several investigations have shown that the phosphatidylinositol 3-kinase/protein kinase B (PI3K/Akt) pathway plays a significant role in a wide range of malignancies

[21–23], and aberrant activation of this system is strongly linked to PCa growth, metastasis, and treatment resistance [24–26]. PI3K is a protein kinase linked to the plasma membrane that is often found downstream of the receptor tyrosine kinase [27]. Once engaged, PI3K catalyzes a number of cascade processes, such as phosphatidylinositol 4,5-bisphosphate (PIP2) phosphorylation, to generate phosphatidylinositol 3-phosphate (PIP3) to activate Akt. The activated Akt can initiate several downstream signaling events via its kinase activity [28,29].

In this study, VGF was found to be elevated in PCa tumor tissues exhibiting malignant behavior as determined through analysis of multiple databases. Additionally, higher levels of VGF were associated with a poor prognosis. Furthermore, VGF showed a strong correlation with the clinical stage and was significantly overexpressed in PCa tissues. Mechanistic investigations revealed that H19 activated PI3K/Akt/ cyclic adenosine monophosphate response element binding protein (CREB) signaling and promoted pancreatic neuroendocrine neoplasms (pNEN) progression by interacting with VGF [30]. The transcriptional regulatory connection between VGF and hypoxia-inducible factor 1 alpha (HIF-1α), as well as the method by which VGF influences PCa cell invasion and migration via the PI3K/Akt pathway, are further explained by this research. This research might clarify the function of VGF in malignancies and offer new avenues for PCa detection and therapy.

2. Materials and Methods

2.1 Bioinformatics Analysis

We used the Gene Expression Omnibus (GEO), a publicly accessible genomics database maintained by the The National Center for Biotechnology Information (NCBI), and the The Cancer Genome Atlas (TCGA) data portal (https://tcga-data.nci.nih.gov/tcga/) to investigate the expression and prognostic significance of VGF in PCa.

We used the UCSC Xena platform (http://xena.ucsc.edu/) and the Gliovis database (http://gliovis.bioinfo.cnio.es/) to investigate the expression and prognostic importance of FTL in glioma. The Cancer Genome Atlas (TCGA), Rembrandt, and the Ivy Prostate Cancer Atlas Project (IVY) datasets normalized *RSEM* gene-level RNA-seq and related clinical data were retrieved from Gliovis. We obtained specific data on postoperative chemotherapy and radiation therapies received by glioma patients from the UCSC Xena platform. Clinical information and normalized mRNA expression [mRNA-array_693, (batch 1)] were also collected from the Chinese Glioma Genome Atlas. The 2021 World Health Organization (WHO) classification of malignancies of the central nervous system classified low-grade glioma as WHO grade I–II and high-grade glioma as WHO grade III-IV [31]. We used JASPAR (https://jaspar.elixir.no/) site predictions to explore the specific mechanisms of action of VGF and HIF-1α.

2.2 Clinical Samples

Between 2022 and 2024, tissue samples were taken from 42 patients with PCa and 21 individuals who had benign prostatic hyperplasia (BPH) at the First Affiliated Hospital of Chongqing Medical University (China). Identities and conditions were anonymized to maintain the integrity of the double-blind review process. In the inpatient department, 37 patients had BPH, and 53 patients had PCa at the same time as plasma samples were taken. Prior to the experiments, specimens were stored in liquid nitrogen to preserve their integrity. All clinical samples were ethically approved by the First Affiliated Hospital of Chongqing Medical University (Approval No. 2022-K275) and conducted in accordance with the Declaration of Helsinki. The patients or legal guardians gave written approval for the biological studies. Every specimen underwent a histological examination and was categorized based on WHO standards and UICC guidelines [32].

2.3 Immunohistochemistry (IHC) Staining

IHC labeling was used to determine the VGF expression levels in tissue samples from 42 PCa and 21 BPH patients. After being deparaffinized in xylene and rehydrated in distilled water and graded alcohol, tissue pieces were pressure-cooked to extract antigens. Then, they were blocked with endogenous peroxidase for 5 min and then incubated at room temperature for 30 min with goat serum. Sections were then incubated with primary antibody for 14 h at 4 °C. VGF nerve growth factor inducible (VGF) (1:300, NBP2-31596, Novus, St. Louis, MO, USA) antibody. Vimentin (1:100, WL01960, Wanlei Bio, Shenyang, Liaoning Province, China) and E-cadherin (1:100, WL00941, Wanlei Bio, Shenyang, Liaoning Province, China). HIF-1α (1:50, A11945, ABclonal, Wuhan, China). The SP Immunohistochemistry Commercial Detection Kit (SP-9000, Beijing Zhongshan Jinqiao Biotechnology Co., Ltd., Beijing, China) was used to perform immunostaining in accordance with the instructions. Following that, they were incubated for 15 min in a working solution of streptavidin/peroxidase complex and then kept for 30 minutes at 37 °C with the kit's biotinylated secondary antibody (1:200, SP-9000; Beijing Zhongshan Jinqiao Biotechnology Co., Ltd.). A diaminobenzidine (DAB) kit (ZLI9018, Beijing Zhongshan Jinqiao Biotechnology Co., Ltd.) was used for the peroxidase staining process. The specimens were stained with hematoxylin staining solution (G1080, Solarbio, Beijing, China) at room temperature for 1 min. Semiquantitative scores were used to calculate staining intensity and immunoreactivity rates. Those classified as negative/weak were regarded as staining negatively for statistical reasons, whereas those with moderate or strong staining were regarded as positive.

2.4 Enzyme-Linked Immunoabsorbent Assay (ELISA)

We quantified plasma VGF levels in patients with prostate disease using an ELISA kit (JM5286H1, Jiangsu Jingmei Biotechnology Co., Ltd., Yancheng, China). Briefly, peripheral blood samples (EDTA-K2 anticoagulant) were collected from all patients and then stored at –80 °C until use. In line with the advice provided by the manufacturer, we used a custom-made ELISA kit (JM5286H1, Jiangsu Jingmei Biotechnology Co., Ltd., Yancheng, China) to quantify plasma *VGF*. The kit was equilibrated to room temperature; the solution was mixed thoroughly to avoid foaming, and the standard was reconstituted with the standard diluent and mixed thoroughly before use. The sample was then diluted 5-fold with the diluent. Next, 50 µL of standard or diluted sample was added to each well and mixed gently by shaking. The plate was covered with a membrane (microplate sealant) and incubated at 37 °C for 30 min. The liquid was discarded, the plate was washed, and the procedure was repeated for six washes. Next, 50 µL of Horseradish peroxidase (HRP) coupling reagent (JM5286H1, Jiangsu Jingmei Biotechnology Co., Ltd.) was added to each well and mixed gently by shaking. The plate was covered with a membrane and incubated at 37 °C for 30 min. After discarding the liquid, the plate was cleaned, and the process was carried out six times. Subsequently, each well was filled with 50 µL of chromogenic solution A and 50 µL of chromogenic solution B and shaken slightly to combine, then allowed to sit at 37 °C (in the dark) for 10 min. After stopping the reaction with 50 µL of stop solution in each well, the optical density was measured at 450 nm for the detection wavelength and 620 nm for the reference wavelength, using a microplate reader (Thermo Varioskan Flash, Thermo Fisher Scientific (China) Co., Ltd., Shanghai, China). A standard curve of optical density measurements was used to determine the amount of VGF protein in each sample.

2.5 Cells, Cell Culture, and Transfection

American Type Culture Collection (ATCC, Manassas, VA, USA) provided the human normal prostate epithelial cells RWPE-1 and the human PCa cells PC3, 22Rv1, and C4-2. All cells were short tandem repeat (STR)-validated to maintain cell line stability. Mycoplasma-free cells were used for all studies. Thermo Fisher Scientific (Boston, Mass., USA) provided 10% FBS, and Beyotime Institute of Biotechnology (Shanghai, China) provided 100 U/mL penicillin/streptomycin as supplements for the RPMI-1640 (Gibco, Thermo Fisher Scientific, MA, USA) medium in which PCa cells were cultivated. The specified keratinocyte-SFM (1×) fluid (Invitrogen, Carlsbad, CA, USA) was used to sustain RWPE-1 cells. Every cell line was cultivated in a humidified environment with 5% CO_2 at 37 °C. Cells were cultivated under constant 1% O hypoxia conditions for *in vitro* hypoxia investigations. The lentiviral *VGF* vector and lentiviral HIF-1α vector were constructed by Beijing Qingke Biotechnology Co., Ltd. The target sequence of *VGF* short hairpin RNA (shRNA) is 5′-CTTCTGCCTTCTGCTGATCAA-3′, and the target sequence of HIF-1α shRNA is 5′-GCCGCTCAATTTATGAATATT-3′. Lentivirus-infected 22Rv1 cells were selected with 1 µg/mL puromycin to establish control sh-NC 22Rv1, sh-*VGF* 22Rv1, and sh-HIF-1α 22Rv1 cells. Overexpression plasmids for *VGF* and HIF-1α were constructed by Hanheng Biotechnology Co., Ltd., and according to the manufacturer's instructions, cells were cultured in 6-well plates and transfected using lip2000 (Invitrogen, Carlsbad, CA, USA). For the subsequent investigation, cells were used 48 h after transfection. Akt activator SC79 (HY-18749, MedChemExpress (MCE), Monmouth Junction, NJ, USA) and docetaxel (HY-B0011, MCE) (Transwell: add to serum medium when inoculating cells; wound healing assays: add to serum-free medium after the cells were injured with a 200 µL pipette tip; WB: serum medium was added after cell attachment).

2.6 Western Blot Assay

After being lysed for around 30 min on ice in RIPA Lysis Buffer (P0013, Beyotime Biotechnology, Shanghai, China), cell samples were centrifuged for 10 min at 12,000 rpm. For each 100 mg tissue, we added 1 mL of RIPA lysate. Using the BCA Assay Kit (Cat. No. P0010, Beyotime Biotechnology), the concentration of proteins was measured. Before loading, protein samples were added to the loading buffer (P0015, Beyotime Biotechnology) and cooked for 4 min in boiling water. In short, the protein was loaded in equal proportions onto 8–12% SDS-PAGE and then transferred to PVDF membranes (Millipore, MA, USA). Then, it was blocked in 5% skim milk for 1 h and incubated with the primary antibody overnight at 4 °C. Membranes were incubated for 1 h at room temperature using a secondary antibody. Protein bands were identified by using an improved chemiluminescence reagent (Cat. No. P10100, Suzhou New Saimei Biotechnology Co., Ltd.). The primary antibodies were as follows: VGF (1:1000; NBP2-31596; Novus); HIF-1α (1:1000; 36169; CST); AKT (1:1000; 9272; CST); p-AKT (1:2000; 4060; CST); PI3K (1:1000; 4292; CST); p-PI3K (1: 1000; 4228; CST); E-cadherin (1:2000; 20874; Proteintech); vimentin (1:1000; 10366; Proteintech); snail 1 (1:3000; WL01863; Wanleibio); and β-actin (1:2000; 20536; Proteintech); β-tubulin (1:2000; 11224; Proteintech). The secondary antibodies are as follows: HRP-conjugated Goat Anti-Mouse IgG (H+L) (1:5000; SA00001-1; Proteintech); HRP-conjugated Goat Anti-Rabbit IgG (H+L) (1:5000; SA00001-2; Proteintech). ImageJ software (1.53j, LOCI, University of Wisconsin, Madison, WI, USA) was used to analyze protein expression.

2.7 Reverse Transcription-Quantitative PCR and Quantitative Real-Time PCR

TRIzol (TaKaRa, Tokyo, Japan) was used to extract total RNA from cell samples, and the Prime Script RT kit (TaKaRa) was used to reverse-transcribe the RNA according to the manufacturer's protocol. PCR was performed using the SYBR Premix Ex Taq™ II Kit (TaKaRa). The $2^{-\Delta\Delta CT}$ technique was used to quantify gene expression. Three replicates of the real-time PCR were run, and the outcomes were adjusted for β-actin. The following are the primer sequences: VGF: (sense: 5′-GGAACTGCGAGATTTCAGTCC-3′, antisense: 5′-GTGCGGGTTCCGTCTCTG-3′); HIF-1α: (sense: 5′-TGATGACCAGCAACTTGAGG-3′, antisense: 5′-CTGGGGCATGGTAAAAGAAA-3′); β-actin: (sense: 5′-GGGACCTGACTGACTACCTC-3′, antisense: 5′-ACGAGACCACCTTCAACTCCAC-3′).

2.8 Transwell and Wound Healing Assays

Cells (2×10^4) were seeded with mixed Matrigel-coated membranes in the upper chamber for Transwell invasion experiments, and cultured in media devoid of fetal bovine serum (FBS). Medium supplemented with 15% FBS was added to the bottom chamber. After a 24-h incubation period, invasive cells were stained with crystal violet, and five visible regions were systematically counted under a microscope at a magnification of 100× (Nikon, Tokyo, Japan). In 6-well plates, cells were sown for wound healing experiments. Once the cells reached 80% confluence, they were injured with a 200 µL pipette tip and continued incubating for 24–48 h. At designated intervals, the wound healing process was examined under a microscope.

2.9 Dual-Luciferase Reporter Assay

In order to study the effect of the interaction between HIF1A and FTL, plasmids of wild-types WT1 and WT2, and mutant types Mut1 and Mut2 containing VGF promoter sequences, were constructed (GS1-21120205; Wuhan Jinkairui Bioengineering Co; WT1: GGTACCGAGCTGATGGGCTTTCTTCTGGGAAAGTCGAGCCACTGATGGAAGCGAGAAGCCACTGCTGGTTATAGAGAGAAAGCACGTGAGTGTGTGTGTAGGGAGGGGGAGGTTAGAAGGAGGGTCAGTGCCAGGAAGAGGTGAGGAGGGGGGCGACTCGAG; WT2: GGTACCCCCCTGTCAGGGGGCTGCCACCCGCACTGCCGATTCGCGGACAGCGCCCGCAGGCGTGCAGATCTGTCCCTCTGCACTCAGGTTCACGCCGTCCTTGGGCGCGTGGTCTCGGGGTGGGGAACCCGGCCCCCTGGTCGGCTCTTGAATCTTCTCGAG; Mut1: GGTACCGAGCTGATGGGCTTTCTTCTGGGAAAGTCGAGCCACTGATGGAAGCGAGAAGCCACTGCTGGTTATAGAGAGAAAACTCACTCGCGTGTGTGTAGGGAGGGGGAGGTTAGAAGGAGGGTCAGTGCCAGGAAGAGGTGAGGAGGGGGGCGACTCGAG; Mut2: GGTACCCCCCTGTCAGGGGGCTGCCACCCGCACTGCCGATTCGCGGACAGCGCCCGCGCACGCCTAGATCTGTCCCTCTGCACTCAGGTTCACGCCGTCCTTGGGCGCGTGGTCTCGGGGTGGGGAACCCGGCCCCCTGGTCGGCTCTTGAATCTTCTCGAG). HEK293T cells were cotransfected with sh-HIF-1α plasmid (or sh-NC plasmid) and WT (or Mut) plasmid and a plasmid containing Renilla luciferase gene. Lipofectamine 2000 (Invitrogen) was used for the transfection process. After 48 h, the luciferase activity was measured using a dual-luciferase reporter system (Promega, Madison, WI). The ratio of firefly to Renilla luciferase activities is known as the relative luciferase activity.

2.10 Chromatin Immunoprecipitation (ChIP)

ChIP was carried out to check for possible binding between HIF1A and the VGF promoter region. For 24 h, 22Rv1 cells were cultivated under hypoxia. Cell Signaling Technologies provided the HIF1A antibody (Cat. No. 36169). The VGF fragment-containing precipitated DNA was subsequently amplified by quantitative PCR. The following primer sequences were used to find the HREs in the VGF promoter: sense, 5′-ACTGATGGAAGCGAGAAG-3′, and antisense, 5′-TCCTGGCACTGACCCT-3′.

2.11 In Vivo Experiments

The supplier of the nude mice was Chongqing Ensiweier Biotechnology Co., Ltd. The experiment Animal Ethics Committee's requirements (Approval No. 2022-K275; the First Affiliated Hospital of Chongqing Medical University) were followed during the care of the mice and the experimental methods. Log phase-grown, stable transfected 22Rv1 cells were produced. The cells were reconstituted in PBS at a density of 5×10^6 cells/100 µL. For the *in vivo* administration of docetaxel therapy, twenty 5-week-old male nude mice, each weighing approximately 15 grams, were randomly divided into four groups, with five mice per group. In the first and second groups, the sh-NC stabilized cell line was injected into the tail vein of the nude mice. Groups III and IV were injected with the sh-VGF-stabilized cell lines into the tail vein of the nude mice. Live imaging for metastasis was conducted four weeks post injection. Nude mice in groups I and III were administered saline (10 mg/kg, once per week) via tail vein injection for three consecutive weeks; nude mice in groups II and IV were injected with docetaxel (10 mg/kg, 1/week) via tail vein for three consecutive weeks. Following tail vein injection, the health and condition of the mice were observed daily [33,34]. After the third week of docetaxel treatment, all nude mice were imaged *in vivo* (IVIS Lumina LT) and then euthanized with 2% pentobarbital (100 mg/kg; IV) plus a high concentration of CO_2. Liver and lung tissue was obtained for sectioning and analysis.

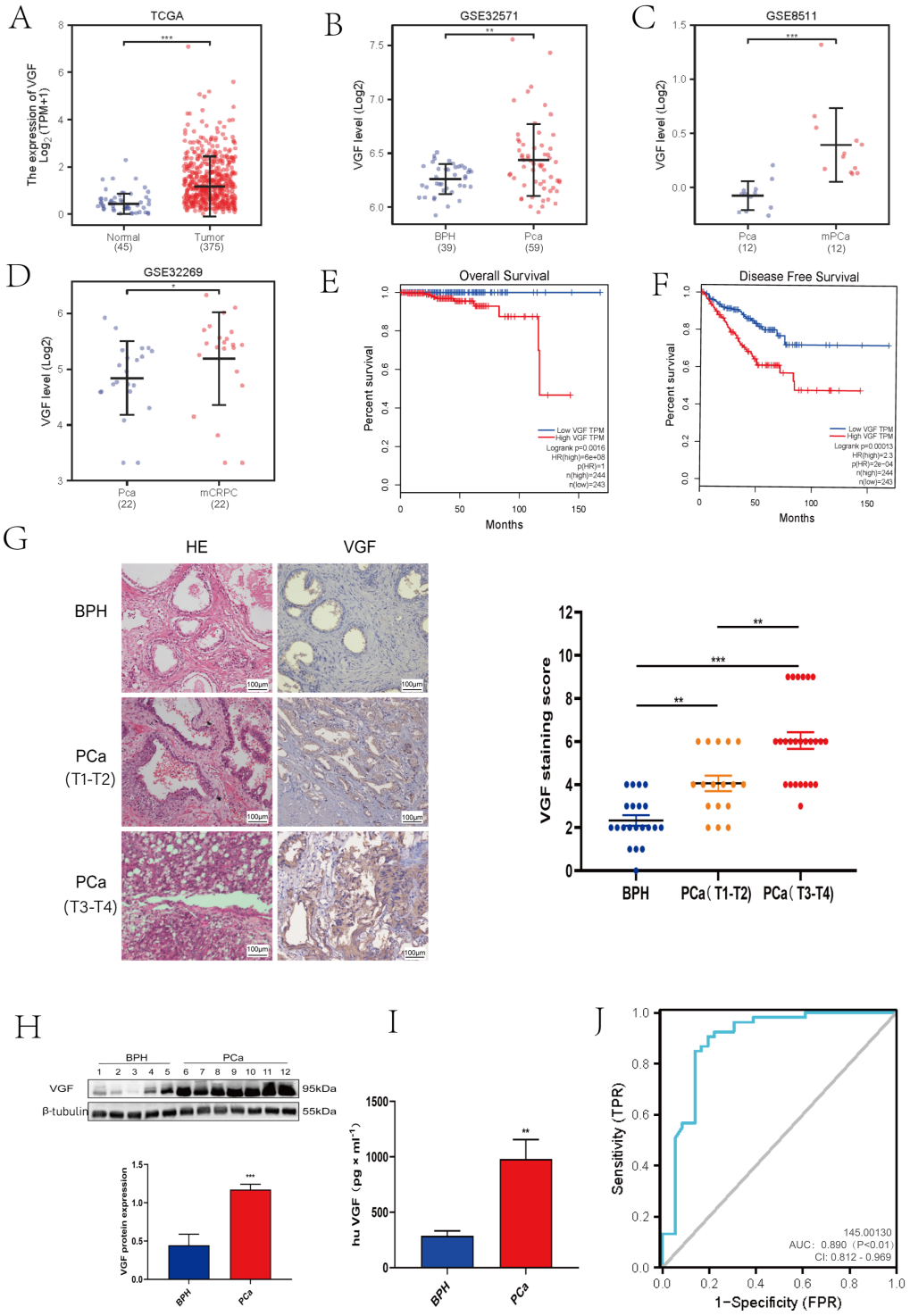

Fig. 1. In prostate cancer (PCa), VGF nerve growth factor inducible (VGF) is overexpressed and related to prognosis. (A) VGF expression in the cancer genome atlas (TCGA) datasets for both PCa and normal prostate. (B) VGF expression in benign prostatic hyperplasia (BPH) and PCa in Gene Expression Omnibus (GEO) datasets. (C) VGF expression in PCa and mPCa in GEO datasets. (D) VGF expression in PCa and mCRPC in GEO datasets. (E) VGF expression survival study across all PCa patients in TCGA. (F) Study of disease-free survival for each PCa patient in TCGA according to VGF expression. (G) Magnification shows representative immunohistochemistry (IHC) and hematoxylin and eosin (H&E) staining for VGF in PCa and BPH samples. Scale bar: 100 μm. (H) The degree of molecular expression in newly obtained PCa tissues and BPH specimens. (**Supplementary Material, Fig. S1A**). (I) The expression of VGF in the plasma of BPH patients and PCa patients. (J) Receiver operating characteristic (ROC) curve plot for prediction of PCa by VGF. *$p < 0.05$; **$p < 0.01$; ***$p < 0.001$.

Table 1. Correlation between VGF expression and clinicopathological factors in PCa patients.

Characteristics	Total no.	VGF			
		Positive (%)	Negative (%)	χ^2	p
Total	42	35 (83)	7 (17)		
Age (years)					
<60	6	4 (67)	2 (33)	0.35	0.554
≥60	36	31 (86)	5 (14)		
Histological stage					
T1–T2	17	11 (65)	6 (35)	5.06	0.024*
T3–T4	25	24 (96)	1 (4)		
Gleason score					
<7	21	14 (67)	7 (33)		0.009*
≥7	21	21 (100)	0 (0)		

VGF, VGF nerve growth factor inducible; PCa, prostate cancer; * Considered statistically significant.

2.12 Statistical Analysis

Each experiment in this investigation was carried out independently at least three times, and SPSS17.0 (Version 17.0.1, SPSS Software, IBM., Armonk, NY, USA) was used to evaluate the data statistically. All data were given as means ± standard deviation (SD). *T*-tests or ANOVA were utilized to conduct statistical comparisons between groups; Bonferroni correction was used for post hoc comparisons, and the hypothesis of normality was tested separately for each group of samples using the Kolmogorov–Smirnov (KS test). The correlation of VGF expression and clinicopathologic factors in PCa patients was assessed using Fisher precision testing and the paired Chi-square test. The fold enrichment method was used for statistical data analysis of ChIP. $p < 0.05$ was deemed to be a significant difference.

3. Results

3.1 VGF is Overexpressed and is Associated with Shorter Survival in PCa

While specific human cancer tissues have been found to overexpress VGF [16,17], the functional involvement of VGF in PCa remains poorly understood. Using the TCGA database and bioinformatic analysis, we examined the expression of VGF and its potential prognostic significance in PCa.

VGF levels in PCa tissue were significantly higher than in normal prostate tissue (Fig. 1A, $p < 0.001$). The analysis from GEO datasets (GSE 32571) also showed the same results (Fig. 1B, $p < 0.01$). Moreover, in the GSE 8511 and GSE 32269 datasets, we found that PCa tissue with metastasis has a higher VGF expression than localized PCa tissues (Fig. 1C,D, $p < 0.001$, $p < 0.05$). Then, using open datasets, we investigated the predictive significance of VGF in PCa. We found that PCa patients in the TCGA datasets who expressed more VGF had worse disease-free survival and overall survival than those who expressed less VGF (Fig. 1E,F, $p < 0.01$).

3.2 Abnormal Levels of VGF in PCa Tissues and Plasma Samples

The results demonstrated that VGF expression was positive in 83.33% (35/42) of PCa samples, compared to 19.05% (4/21) in the BPH samples (Fig. 1G, $p < 0.01$).

Next, the relationship between VGF expression and the clinicopathological characteristics of PCa patients was examined. These results showed a significant relationship between the histological stage, Gleason score, and VGF expression (Table 1). The VGF nerve growth factor inducible (VGF) protein levels in 7 fresh PCa and 5 fresh BPH surgical tissue specimens were found to be considerably greater in the PCa tissue than the BPH tissues (Fig. 1H, $p < 0.001$). The relative expression of VGF in plasma samples from 53 PCa patients and 37 BPH patients was assessed using ELISA to better assess the function of VGF in PCa. The PCa patients showed higher expression of VGF compared to the BPH patients (Fig. 1I, $p < 0.01$). The current study further investigated the potential of VGF as a diagnostic biomarker for PCa through the analysis of the receiver operating characteristic (ROC) curve. With a 95% confidence interval [CI] = 0.812–0.969 and an area under the curve (AUC) of 0.890 (Fig. 1J, $p < 0.01$), it appears that VGF may be a useful tool for PCa diagnosis. When combined, our results suggested that VGF may function as a prognostic biomarker and be connected to PCa development.

3.3 VGF Knockdown Suppresses PCa Metastasis

Consistent with the observation that VGF expression is increased in human PCa tissue, PCa cell lines (C4-2, PC3, and 22Rv1) exhibited significantly higher levels of VGF expression in both mRNA and protein levels when compared to the normal prostate epithelial cell line RWPE-1 (Fig. 2A,B, $p < 0.05$).

Lentiviral vectors expressing VGF shRNA (sh-VGF) or control shRNA (sh-NC) were created to knock down the expression of VGF in 22Rv1 cells in order to ascertain if VGF plays a significant role in PCa development

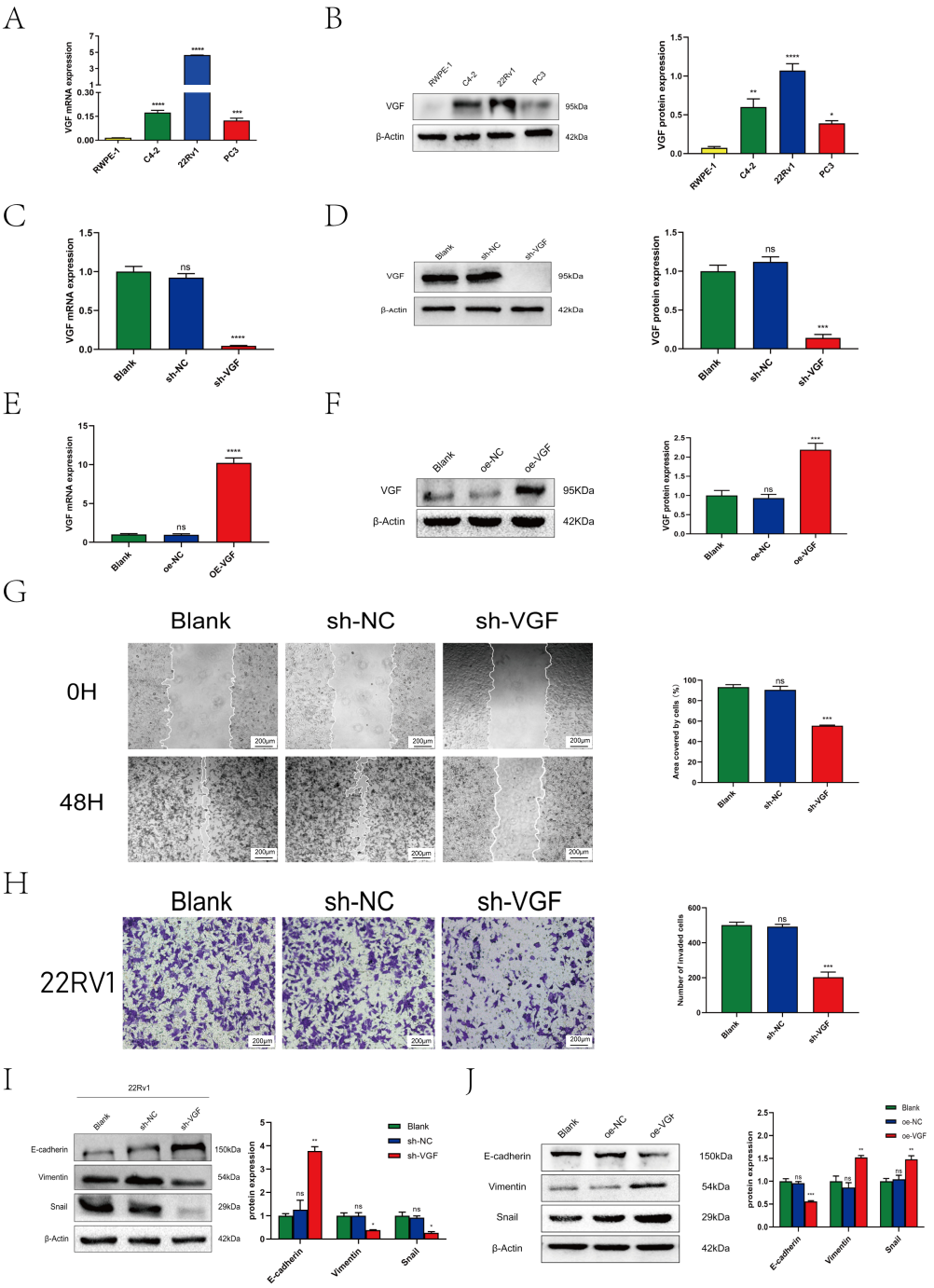

Fig. 2. *VGF* knockdown suppresses PCa metastasis. (A) Expression of *VGF* in RWPE-1, C4-2, 22Rv1, and PC3 cells was detected by quantitative real-time PCR (RT-qPCR). (B) Expression of VGF in RWPE-1, C4-2, 22Rv1, and PC3 cells was detected by western blot. (**Supplementary Material, Fig. S1B**). (C) Expression of *VGF* in blank, sh-negative control (sh-NC), and sh-VGF cells was detected by RT-qPCR. (D) Expression of VGF in blank, shNC, and sh-VGF cells was detected using western blot. (**Supplementary Material, Fig. S1C**). (E) Expression of *VGF* in blank, oe-NC, and oe-VGF cells was detected by RT-qPCR. (F) Expression of VGF in blank, oe-NC, and oe-VGF cells was detected by western blot. (**Supplementary Material, Fig. S1D**). (G,H) The wound-healing test and Transwell assays were used to assess the effects of sh-VGF on 22Rv1 cell migration and invasion. Scale bar: 200 μm. (I) Effects of sh-VGF on the expression of migration-related genes. (**Supplementary Material, Fig. S1E**). (J) Effects of oe-VGF on the expression of migration-related genes. (**Supplementary Material, Fig. S1F**). ns, not significant; *$p < 0.05$; **$p < 0.01$; ***$p < 0.001$; ****$p < 0.0001$.

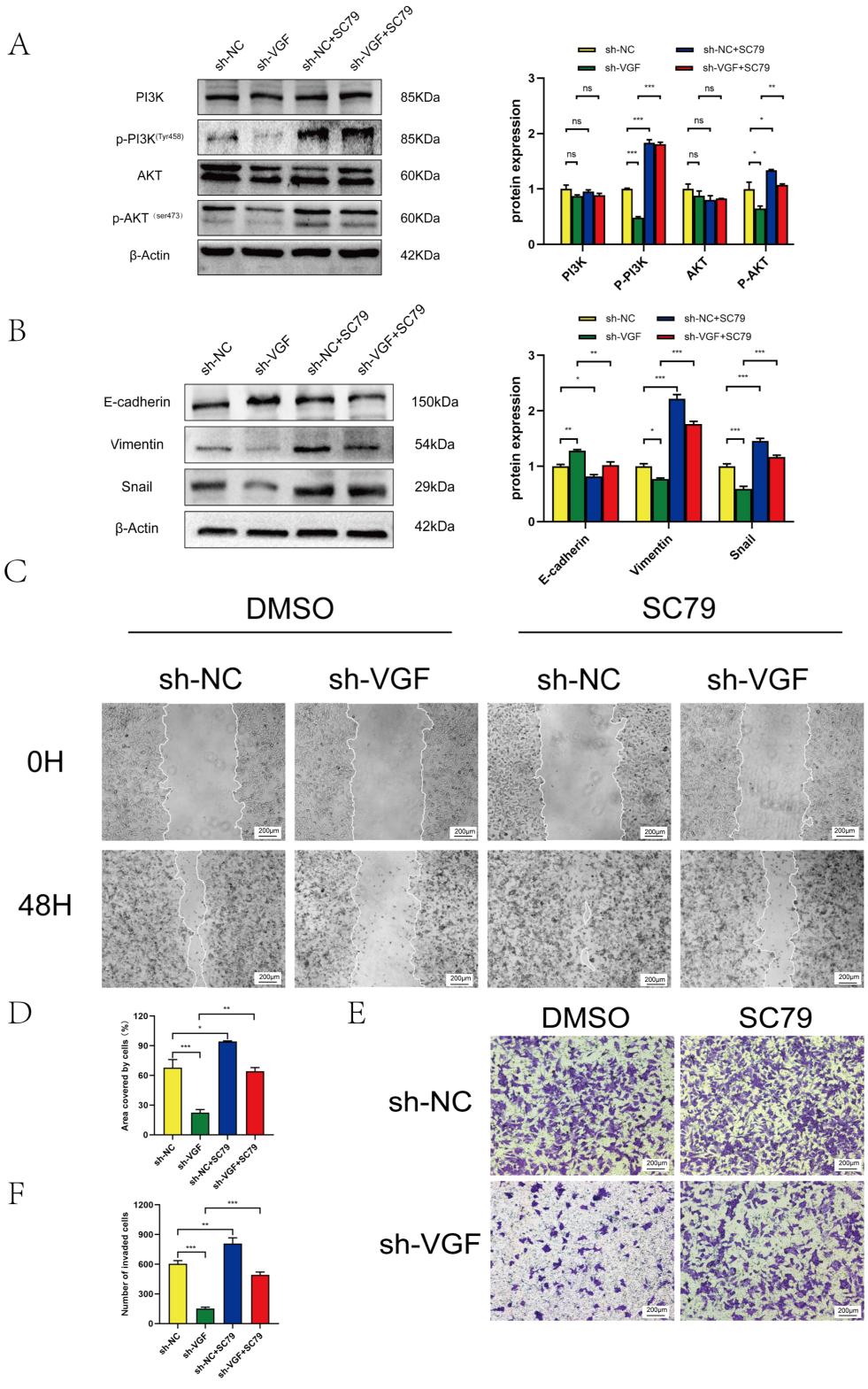

Fig. 3. PI3K/Akt signaling is involved in downstream events of VGF activation. (A) Effects of SC79 and VGF together on PI3K/Akt signaling expression. (**Supplementary Material, Fig. S1G**). (B) Effects of SC79 and VGF together on the expression of genes linked to migration. (**Supplementary Material, Fig. S1H**). (C–F) Changes in 22Rv1 cell migration and invasion after SC79 sh-VGF administration were identified using Transwell assays and the wound-healing test. ns, not significant; scale bar: 200 μm; *$p < 0.05$; **$p < 0.01$; ***$p < 0.001$; ns, not significant.

(Fig. 2C,D, $p < 0.0001$, $p < 0.001$). Simultaneously, overexpressed VGF (oe-VGF) and a control plasmid (oe-NC) were created to boost VGF expression in C4-2 cells (Fig. 2E,F, $p < 0.0001$, $p < 0.001$). To investigate whether sh-VGF contributes to PCa formation, 22Rv1 cell invasion and migration were investigated using Transwell and wound-healing assays. The capacity for invasion and migration of 22Rv1 cells was diminished with VGF knockdown (Fig. 2G,H, $p < 0.001$). Consistent with the above results, western blot investigations indicated that knocking down VGF affected the amounts at which proteins linked to invasion and metastasis are expressed. In 22Rv1 cells, there was an increase in E-cadherin expression and a decrease in vimentin and snail levels (Fig. 2I, $p < 0.05$). In addition, opposing results were observed in the C4-2 cells overexpressing VGF (Fig. 2J, $p < 0.01$).

3.4 PI3K/Akt Signaling is Involved in Downstream Events of VGF Activation

VGF has been reported to enhance PI3K kinase activity in human pancreatic neuroendocrine neoplasms [8]. Therefore, we tested the influence of VGF on activation of the PI3K/Akt signaling pathway by western blot. Western blot showed that phospho-PI3K p85 (Tyr458) and phospho-Akt (Ser473) were greatly inhibited in 22Rv1 cells treated with sh-VGF (Fig. 3A, $p < 0.001$, $p < 0.05$). In contrast, the total amount of PI3K and Akt protein remained unchanged (Fig. 3A). These results suggested that VGF affected the PI3K/Akt pathway. To further estimate the effect of the PI3K pathway on VGF knockdown cells, 22Rv1 cells were treated with the Akt activator SC79 (4 µg/mL). Western blot confirmed that phosphorylation levels of PI3K and Akt were restored by the addition of SC79 in VGF knockdown cells (Fig. 3A, $p < 0.01$).

Next, we examined the role of the PI3K/Akt pathway in 22Rv1 cells transfected with sh-NC or sh-VGF using the wound-healing test, Transwell assay, and western blot analysis. As expected, the capacity of VGF knockdown 22Rv1 cells for invasion and migration was restored by SC79 treatment (Fig. 3B–F, $p < 0.01$). These findings suggest that VGF influences PI3K/Akt signaling, which in turn affects PCa cell invasion and metastasis.

3.5 sh-VGF Combined with Docetaxel can Further Inhibit PCa Metastasis

Docetaxel is a commonly used chemotherapy drug for mPCa, and long-term use will lead to resistance in most patients [35–37]. In clinical practice, docetaxel is often used in combination with targeted drugs [38,39]. We assessed whether targeted knockdown of VGF strengthens docetaxel's inhibitory effect on PCa cell metastasis. Compared with the single-treatment group, the results of wound-healing assays and Transwell assays indicated that the combined-treatment group with targeted knockdown of VGF and docetaxel showed more significant inhibition of the invasion and metastasis of PCa cells (Fig. 4A–D, $p < 0.01$).

To construct a tumor-metastasis model, 22Rv1 cells were injected into the tail vein of male nude mice in order to study the impact of VGF on PCa metastasis *in vivo*. Four weeks later, the nude mice were randomized to receive either saline or docetaxel tail vein injections (Fig. 5A) [40].

As shown in Fig. 5, relative to the sh-NC group, *in vivo* imaging of both the sh-VGF and docetaxel groups revealed that the degree of metastasis in nude mice was less, and the lung tissue stained with H&E showed a fewer number of malignant nodules. The degree of metastases in the combination therapy group was much less than in the single-factor treatment group (Fig. 5B–D, $p < 0.05$). The results indicated that VGF knockdown could limit PCa metastasis, and the inhibitory impact is higher when paired with docetaxel [33,34].

3.6 Hypoxia-Induced VGF in an HIF-1α-Dependent Manner

A well-established feature of clinical PCa associated with poorer prognosis is hypoxia [41,42]. To explore whether hypoxia can affect the expression of VGF, we placed 22Rv1 cells and C4-2 cells under hypoxic conditions [43]. The development of hypoxia in 22Rv1 and C4-2 cells was observed to cause an increase in the amounts of VGF mRNA and protein, as well as an increase in the protein level of hypoxia-inducible factor-1alpha (HIF-1α), according to findings from the western blot and q-PCR (Fig. 6A–C, $p < 0.05$).

We also constructed a plasmid to knock down HIF-1α. After the targeted suppression of HIF-1α in PCa cells, the amounts of VGF protein and mRNA decreased. In order to explore the specific mechanism of action of VGF and HIF-1α, we found two hypoxia response elements on the VGF promoter using JASPAR website prediction (Fig. 6D). We used luciferase and ChIP experiments to determine whether HIF-1α directly binds to the VGF promoter. We found, using a dual luciferase reporter experiment, that WT1's luciferase activity was significantly higher in hypoxia than in a normoxic environment, whereas this phenomenon was not observed in WT2 (Fig. 6E, $p < 0.001$), indicating that the transcription factor HIF-1 binds primarily through the HRE1 site on the VGF promoter. Additionally, we found that knocking down HIF-1 decreased the luciferase activity of WT1 (Fig. 6F, $p < 0.001$). By using a chromatin immunoprecipitation test, we demonstrated that HIF1 attaches to an area of the VGF promoter (Fig. 6G, $p < 0.05$). Consequently, we found that HIF-1 controls VGF transcription as a transcription factor. Our findings indicate that, as a transcription factor, HIF-1 could bind to promoter regions on the VGF gene and regulate the transcription of VGF.

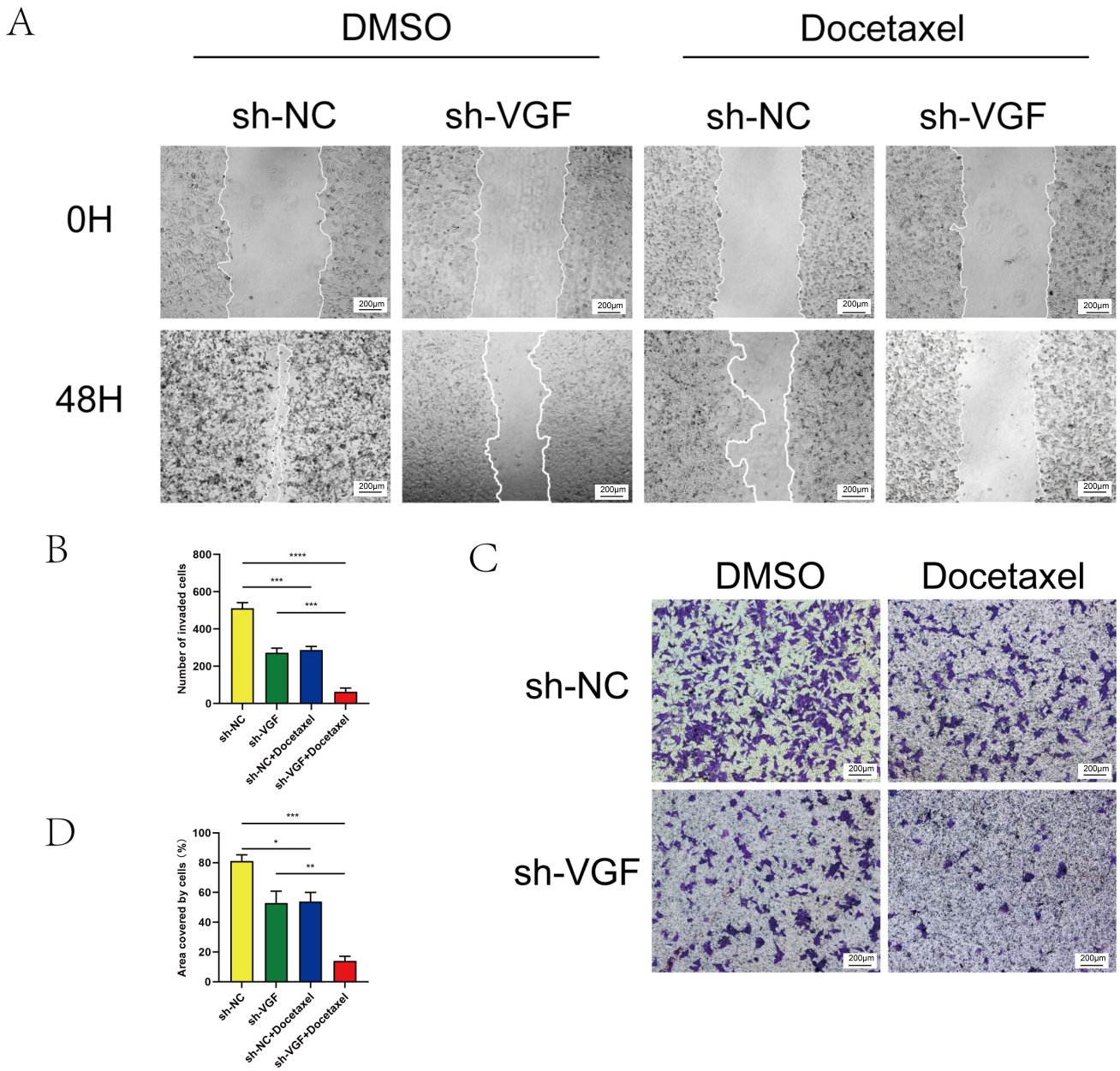

Fig. 4. sh-VGF combined with docetaxel can further inhibit PCa metastasis *in vitro*. (A,B) Changes in 22Rv1 cell migration after docetaxel + sh-VGF administration were identified using a wound-healing test (scale bar: 200 μm). (C,D) Changes in 22Rv1 cell invasion under docetaxel + sh-VGF treatment were determined by Transwell assay (scale bar: 200 μm). *$p < 0.05$; **$p < 0.01$; ***$p < 0.001$; ****$p < 0.0001$.

4. Discussion

Although VGF has been documented to enhance the formation of various malignancies, its involvement in prostate adenocarcinogenesis is little understood. Recent research has demonstrated that high VGF expression is associated with chemoresistance and silencing VGF-induced BMF and BCL2L11 expression and rendered lung cancer cells sensitive to chemotherapy drugs [44]. The PI3K/Akt signaling pathway is one of the most frequently dysregulated signaling pathways found in cancer patients [45] and is essential for carcinogenesis, progression, and treatment sensitivity [46,47]. In addition, earlier research [48] demonstrated that VGF genes are related to the prognosis of radiotherapy-treated PCa.

In the present study, we investigated the expression of VGF in PCa. By integrating databases and clinical samples, our study revealed a strong and positive association between the expression of VGF in PCa tissue and blood, which was supported by cellular experiments. Akt activator SC79 specifically binds to the PH domain of Akt and can cross the plasma-brain barrier, activating Akt in the cy-

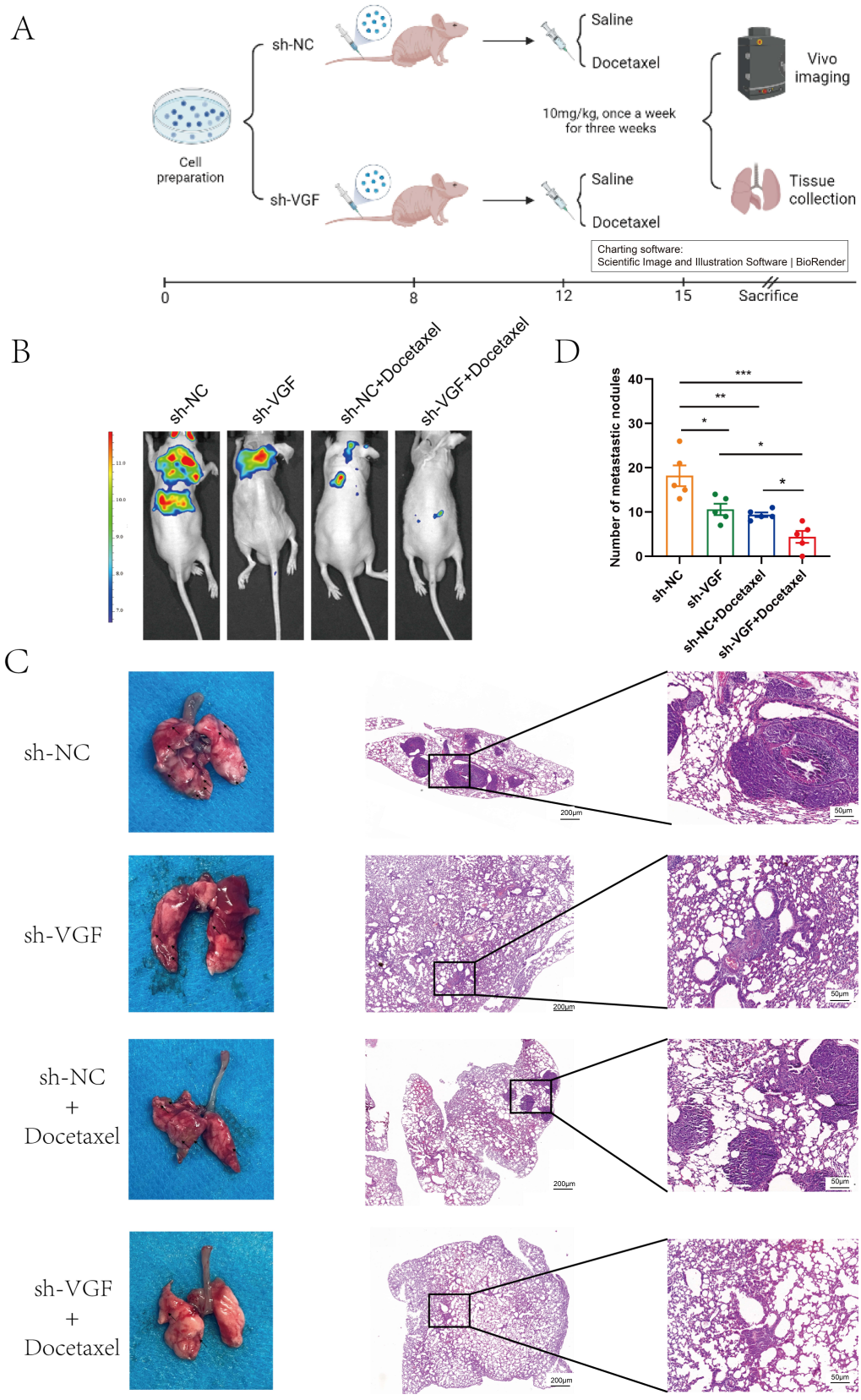

Fig. 5. sh-VGF combined with docetaxel can further inhibit PCa metastasis *in vivo*. (A) Construction of tail vein transfer 324 model in nude mice. (B) *In vivo* tumor imaging. (C,D) H&E staining suggests the extent of cancer cell metastasis in the 325 lungs of nude mice (scale bar: 200 μm; scale bar: 50 μm). *$p < 0.05$; **$p < 0.01$; ***$p < 0.001$.

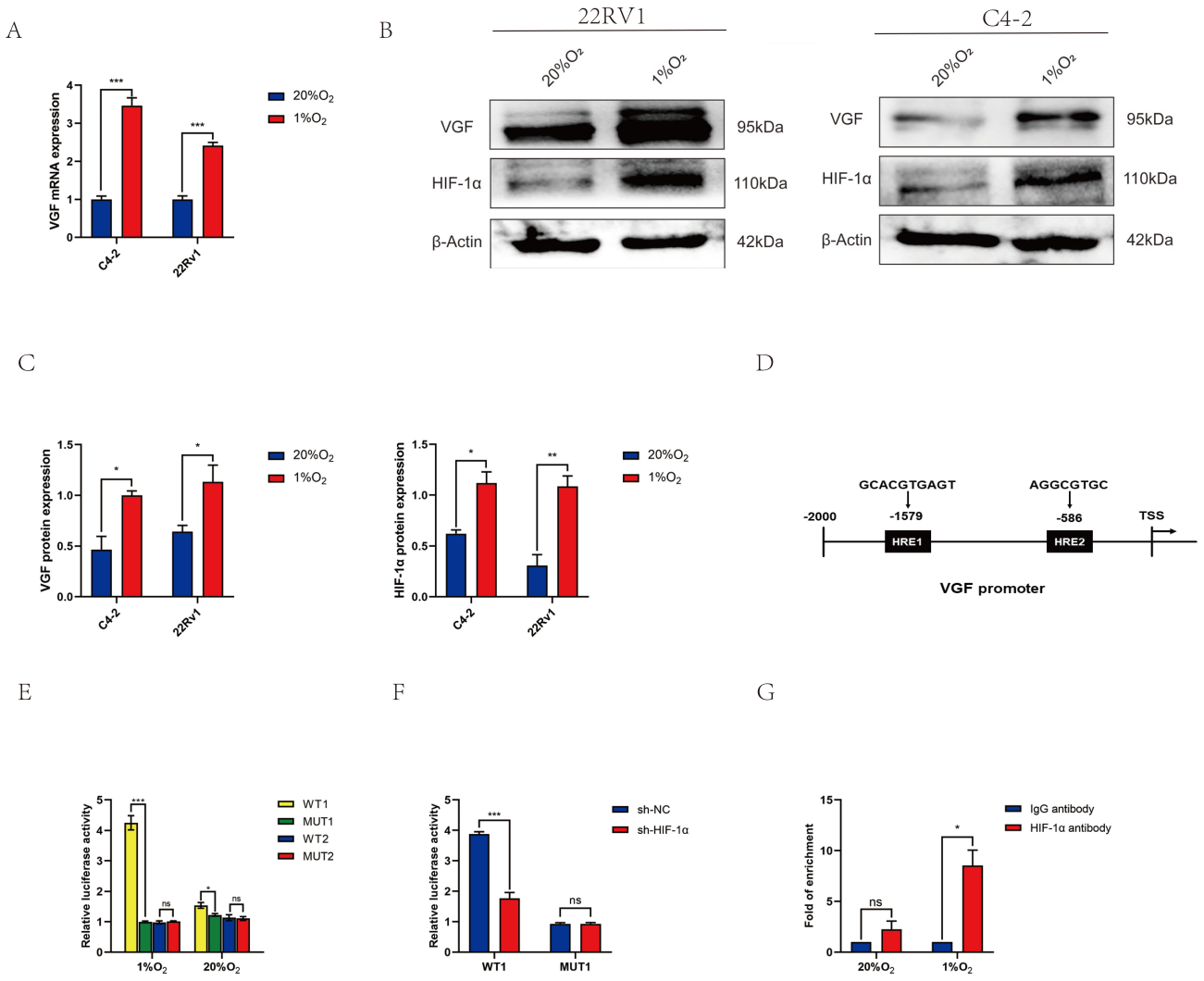

Fig. 6. Hypoxia-induced VGF in an HIF-1α-dependent manner. (A) Variations in mRNA levels of *VGF* in 22Rv1 cells and C4-2 cells under 1% and 20% oxygen environments. (B,C) Variations in protein levels of VGF in 22Rv1 cells and C42 cells under 1% and 20% oxygen environments. (**Supplementary Material, Fig. S1I-J**). (D) Graphs showing the putative hypoxia response elements (HREs) and the mutant VGF promoter in the same region. (E,F) Fluorescein levels after co-transfection of WT1 or WT2 plasmids with Renilla luciferase reporter plasmids. (G) A sample of HIF1A's ChIP binding to the VGF promoter at 1% and 20% oxygen. ns, not significant; $*p < 0.05$; $**p < 0.01$; $***p < 0.001$.

toplasm and inhibiting Akt membrane translocation. In this work, we also found that VGF depletion enhanced the invasive metastasis of PCa cells and that the PI3k/Akt pathway regulates the start and progression of PCa. Our findings indicate that VGF depletion influences the phosphorylation of the PI3k/Akt pathway to further decrease PCa cell invasion and metastasis. Docetaxel is a commonly used chemotherapeutic agent for mPCa [38]. Docetaxel is a semi-synthetic analog of paclitaxel that has antitumor activity by attenuating the effects of bcl-2 and bcl-xL gene expression, blocking the G2/M cell cycle, and causing apoptosis. Our analysis demonstrated that VGF silencing, in combination with docetaxel treatment, further inhibited PCa invasion and metastasis. The *in vitro* experimental results were consistent with our *in vivo* results in demonstrating that VGF silencing and docetaxel treatment, alone or in combination, significantly decreased the metastatic capacity of 22Rv1 PCa cells in a systemic metastasis assay in nude mice. In addition, hypoxia is strongly associated with PCa metastasis, and our present study indicated that HIF-1α, as a transcription factor, combined with HRE1 on the VGF promoter to promote the transcription of VGF; this influences the production of VGF, which in turn influences the invasive metastasis of PCa cells.

However, the present study had several limitations. PCa development is associated with anomalies in numerous signaling pathways. Our current work only investigated the VGF influence on the invasive metastasis of PCa cells via the PI3k/Akt signaling pathway. More research is required to discover whether VGF also affects other im-

portant signaling pathways and contributes to the spread of PCa. At the same time, the influence of VGF on the invasive metastasis of PCa cells via the PI3k/Akt signaling pathway should be explored in a variety of cell lines. However, due to time and financial constraints, the present study was performed only in one cell line, 22RV1. In addition, our findings revealed that VGF silencing, in conjunction with docetaxel treatment, further decreased the invasive metastasis of PCa cells. However, more validation is required to evaluate whether VGF influences drug resistance in patients with CRPC. Overall, our findings demonstrated that VGF influences the aggressive spread of PCa and that VGF expression is also related to a hypoxic tumor microenvironment. In addition, suppressing VGF in conjunction with pharmacological agents may decrease the invasive metastasis of PCa cells in a synergistic manner. Therefore, our research clarified the possible mechanisms by which VGF promotes metastasis and provided a scientific rationale for VGF as a predictor.

5. Conclusion

We investigated how VGF affected PCa invasion and metastasis: the degree of malignancy in PCa was closely linked with aberrantly high expression of VGF. A hypoxic environment further induced the abnormally high expression of VGF. It was shown that the knockdown of VGF greatly inhibited phosphorylation and phosphorylated Akt in cells and reduced cell invasion and migration, and the addition of Akt activator SC79 restored the phosphorylation level as well as the cell invasion and migration ability. This shows that VGF affects the invasion and metastasis of PCa cells via the PI3K/Akt pathway. In studies conducted *in vivo* and *in vitro*, the combination of sh-VGF with docetaxel treatment more effectively suppressed the metastatic effect of PCa cells. Therefore, sh-VGF and docetaxel treatment inhibited the metastasis of PCa cells more significantly.

Availability of Data and Materials

The data supporting the findings of this study are available within the article and its supplementary materials. Further inquiries can be directed to the corresponding author, Ou Liping.

Author Contributions

LLW and TZ developed the study and contributed equally to this work. YNQ, YYW, TL, and YBZ undertook the data collection and analysis. LLW and TZ drafted the manuscript. CLL, XHW, TMC, and LPO conceptualized and investigated the study and critically reviewed the manuscripts. All authors read and approved the final version of the manuscript. All authors contributed to editorial changes in the manuscript. All authors have participated sufficiently in the work and agreed to be accountable for all aspects of the work.

Ethics Approval and Consent to Participate

The study was approved by the Ethics Committee of the Chongqing Medical University (Approval No. 2022-K275) for both animals and humans, and all participants were asked to provide written informed consent. The study was carried out in accordance with the guidelines of the Declaration of Helsinki.

Acknowledgment

Not applicable.

Funding

This work was supported by the National Natural Science Foundation of China (no. 82202580); Chongqing Natural Science Foundation (no. CSTB2022NSCQ-BHX0686); Chongqing Natural Science Foundation (no. CSTB2024NSCQ-MSX0141) and Chongqing Overseas Chinese Returned Entrepreneurship and Innovation Support Program of P. R. China (Grant No. cx2021095).

Conflict of Interest

The authors declare no conflict of interest.

Supplementary Material

Supplementary material associated with this article can be found, in the online version, at https://doi.org/10.31083/FBL25522.

References

[1] Bergengren O, Pekala KR, Matsoukas K, Fainberg J, Mungovan SF, Bratt O, *et al*. 2022 Update on Prostate Cancer Epidemiology and Risk Factors-A Systematic Review. European Urology. 2023; 84: 191–206. https://doi.org/10.1016/j.eururo.2023.04.021.

[2] Siegel RL, Miller KD, Fuchs HE, Jemal A. Cancer statistics, 2022. CA: a Cancer Journal for Clinicians. 2022; 72: 7–33. https://doi.org/10.3322/caac.21708.

[3] Abrams P. Benign prostatic hyperplasia: The term BPH is misused. BMJ (Clinical Research Ed.). 2008; 336: 405. https://doi.org/10.1136/bmj.39493.447361.1F.

[4] Chughtai B, Forde JC, Thomas DDM, Laor L, Hossack T, Woo HH, *et al*. Benign prostatic hyperplasia. Nature Reviews. Disease Primers. 2016; 2: 16031. https://doi.org/10.1038/nrdp.2016.31.

[5] Zhou Q, Chen X, Yao K, Zhang Y, He H, Huang H, *et al*. TSPAN18 facilitates bone metastasis of prostate cancer by protecting STIM1 from TRIM32-mediated ubiquitination. Journal of Experimental & Clinical Cancer Research. 2023; 42: 195. https://doi.org/10.1186/s13046-023-02764-4.

[6] Li Z, Tao Y, Gao Z, Peng S, Lai Y, Li K, *et al*. SYTL2 promotes metastasis of prostate cancer cells by enhancing FSCN1-mediated pseudopodia formation and invasion. Journal of Translational Medicine. 2023; 21: 303. https://doi.org/10.1186/s12967-023-04146-y.

[7] Sekhoacha M, Riet K, Motloung P, Gumenku L, Adegoke A, Mashele S. Prostate Cancer Review: Genetics, Diagnosis, Treatment Options, and Alternative Approaches. Molecules. 2022; 27: 5730. https://doi.org/10.3390/molecules27175730.

[8] Achard V, Putora PM, Omlin A, Zilli T, Fischer S. Metastatic Prostate Cancer: Treatment Options. Oncology. 2022; 100: 48–59. https://doi.org/10.1159/000519861.

[9] Sweeney CJ, Martin AJ, Stockler MR, Begbie S, Chi KN, Chowdhury S, *et al*. Overall Survival of Men with Metachronous Metastatic Hormone-sensitive Prostate Cancer Treated with Enzalutamide and Androgen Deprivation Therapy. European Urology. 2021; 80: 275–279. https://doi.org/10.1016/j.eururo.2021.05.016.

[10] Cornford P, van den Bergh RCN, Briers E, Van den Broeck T, Cumberbatch MG, De Santis M, *et al*. EAU-EANM-ESTRO-ESUR-SIOG Guidelines on Prostate Cancer. Part II-2020 Update: Treatment of Relapsing and Metastatic Prostate Cancer. European Urology. 2021; 79: 263–282. https://doi.org/10.1016/j.eururo.2020.09.046.

[11] Ge R, Wang Z, Montironi R, Jiang Z, Cheng M, Santoni M, *et al*. Epigenetic modulations and lineage plasticity in advanced prostate cancer. Annals of Oncology. 2020; 31: 470–479. https://doi.org/10.1016/j.annonc.2020.02.002.

[12] Levi A, Eldridge JD, Paterson BM. Molecular cloning of a gene sequence regulated by nerve growth factor. Science. 1985; 229: 393–395. https://doi.org/10.1126/science.3839317.

[13] Wang Y, Qin X, Han Y, Li B. VGF: A prospective biomarker and therapeutic target for neuroendocrine and nervous system disorders. Biomedicine & Pharmacotherapy. 2022; 151: 113099. https://doi.org/10.1016/j.biopha.2022.113099.

[14] Lin WJ, Zhao Y, Li Z, Zheng S, Zou JL, Warren NA, *et al*. An increase in VGF expression through a rapid, transcription-independent, autofeedback mechanism improves cognitive function. Translational Psychiatry. 2021; 11: 383. https://doi.org/10.1038/s41398-021-01489-2.

[15] Thakker-Varia S, Alder J. Neuropeptides in depression: role of VGF. Behavioural Brain Research. 2009; 197: 262–278. https://doi.org/10.1016/j.bbr.2008.10.006.

[16] Wu Z, Jiao M, Shu C, Zhang S, Wang J, Pu J, *et al*. Integrin $\alpha V\beta 1$-activated PYK2 promotes the progression of non-small-cell lung cancer via the STAT3-VGF axis. Cell Communication and Signalin. 2024; 22: 313. https://doi.org/10.1186/s12964-024-01639-1.

[17] Wang J, Chen Y, Li X, Zou X. Perineural Invasion and Associated Pain Transmission in Pancreatic Cancer. Cancers. 2021; 13: 4594. https://doi.org/10.3390/cancers13184594.

[18] Gabanella F, Maftei D, Colizza A, Rullo E, Riminucci M, Pasqualucci E, *et al*. Reduced expression of secretogranin VGF in laryngeal squamous cell carcinoma. Oncology Letters. 2023; 27: 37. https://doi.org/10.3892/ol.2023.14170.

[19] Chou CH, Yen CH, Liu CJ, Tu HF, Lin SC, Chang KW. The upregulation of VGF enhances the progression of oral squamous carcinoma. Cancer Cell International. 2024; 24: 115. https://doi.org/10.1186/s12935-024-03301-9.

[20] Seifert M, Peitzsch C, Gorodetska I, Börner C, Klink B, Dubrovska A. Network-based analysis of prostate cancer cell lines reveals novel marker gene candidates associated with radioresistance and patient relapse. PLoS Computational Biology. 2019; 15: e1007460. https://doi.org/10.1371/journal.pcbi.1007460.

[21] Miricescu D, Totan A, Stanescu-Spinu II, Badoiu SC, Stefani C, Greabu M. PI3K/AKT/mTOR Signaling Pathway in Breast Cancer: From Molecular Landscape to Clinical Aspects. International Journal of Molecular Sciences. 2020; 22: 173. https://doi.org/10.3390/ijms22010173.

[22] Tian LY, Smit DJ, Jücker M. The Role of PI3K/AKT/mTOR Signaling in Hepatocellular Carcinoma Metabolism. International Journal of Molecular Sciences. 2023; 24: 2652. https://doi.org/10.3390/ijms24032652.

[23] Baghery Saghchy Khorasani A, Pourbagheri-Sigaroodi A, Pirsalehi A, Safaroghli-Azar A, Zali MR, Bashash D. The PI3K/Akt/mTOR signaling pathway in gastric cancer; from oncogenic variations to the possibilities for pharmacologic interventions. European Journal of Pharmacology. 2021; 898: 173983. https://doi.org/10.1016/j.ejphar.2021.173983.

[24] Pungsrinont T, Kallenbach J, Baniahmad A. Role of PI3K-AKT-mTOR Pathway as a Pro-Survival Signaling and Resistance-Mediating Mechanism to Therapy of Prostate Cancer. International Journal of Molecular Sciences. 2021; 22: 11088. https://doi.org/10.3390/ijms222011088.

[25] Yue S, Li J, Lee SY, Lee HJ, Shao T, Song B, *et al*. Cholesteryl ester accumulation induced by PTEN loss and PI3K/AKT activation underlies human prostate cancer aggressiveness. Cell Metabolism. 2014; 19: 393–406. https://doi.org/10.1016/j.cmet.2014.01.019.

[26] Mateo J, Seed G, Bertan C, Rescigno P, Dolling D, Figueiredo I, *et al*. Genomics of lethal prostate cancer at diagnosis and castration resistance. The Journal of Clinical Investigation. 2020; 130: 1743–1751. https://doi.org/10.1172/JCI132031.

[27] Shorning BY, Dass MS, Smalley MJ, Pearson HB. The PI3K-AKT-mTOR Pathway and Prostate Cancer: At the Crossroads of AR, MAPK, and WNT Signaling. International Journal of Molecular Sciences. 2020; 21: 4507. https://doi.org/10.3390/ijms21124507.

[28] Manning BD, Toker A. AKT/PKB Signaling: Navigating the Network. Cell. 2017; 169: 381–405. https://doi.org/10.1016/j.cell.2017.04.001.

[29] Shen Q, Han Y, Wu K, He Y, Jiang X, Liu P, *et al*. MrgprF acts as a tumor suppressor in cutaneous melanoma by restraining PI3K/Akt signaling. Signal Transduction and Targeted Therapy. 2022; 7: 147. https://doi.org/10.1038/s41392-022-00945-9.

[30] Ji M, Yao Y, Liu A, Shi L, Chen D, Tang L, *et al*. lncRNA H19 binds VGF and promotes pNEN progression via PI3K/AKT/CREB signaling. Endocrine-related Cancer. 2019; 26: 643–658. https://doi.org/10.1530/ERC-18-0552.

[31] Louis DN, Perry A, Wesseling P, Brat DJ, Cree IA, Figarella-Branger D, *et al*. The 2021 WHO Classification of Tumors of the Central Nervous System: a summary. Neuro-Oncology. 2021; 23: 1231–1251. https://doi.org/10.1093/neuonc/noab106.

[32] Moch H, Amin MB, Berney DM, Compérat EM, Gill AJ, Hartmann A, *et al*. The 2022 World Health Organization Classification of Tumours of the Urinary System and Male Genital Organs-Part A: Renal, Penile, and Testicular Tumours. European Urology. 2022; 82: 458–468. https://doi.org/10.1016/j.eururo.2022.06.016.

[33] Zhong W, Wu K, Long Z, Zhou X, Zhong C, Wang S, *et al*. Gut dysbiosis promotes prostate cancer progression and docetaxel resistance via activating NF-κB-IL6-STAT3 axis. Microbiome. 2022; 10: 94. https://doi.org/10.1186/s40168-022-01289-w.

[34] Lu X, Yang F, Chen D, Zhao Q, Chen D, Ping H, *et al*. Quercetin reverses docetaxel resistance in prostate cancer via androgen receptor and PI3K/Akt signaling pathways. International Journal of Biological Sciences. 2020; 16: 1121–1134. https://doi.org/10.7150/ijbs.41686.

[35] Smith MR, Hussain M, Saad F, Fizazi K, Sternberg CN, Crawford ED, *et al*. Darolutamide and Survival in Metastatic, Hormone-Sensitive Prostate Cancer. The New England Journal of Medicine. 2022; 386: 1132–1142. https://doi.org/10.1056/NEJMoa2119115.

[36] Kyriakopoulos CE, Chen YH, Carducci MA, Liu G, Jarrard DF, Hahn NM, *et al*. Chemohormonal Therapy in Metastatic Hormone-Sensitive Prostate Cancer: Long-Term Survival Analysis of the Randomized Phase III E3805 CHAARTED Trial. Journal of Clinical Oncology. 2018; 36: 1080–1087. https://doi.org/10.1200/JCO.2017.75.3657.

[37] Swami U, McFarland TR, Nussenzveig R, Agarwal N. Ad-

vanced Prostate Cancer: Treatment Advances and Future Directions. Trends in Cancer. 2020; 6: 702–715. https://doi.org/10.1016/j.trecan.2020.04.010.

[38] Gravis G, Boher JM, Joly F, Soulié M, Albiges L, Priou F, *et al*. Androgen Deprivation Therapy (ADT) Plus Docetaxel Versus ADT Alone in Metastatic Non castrate Prostate Cancer: Impact of Metastatic Burden and Long-term Survival Analysis of the Randomized Phase 3 GETUG-AFU15 Trial. European Urology. 2016; 70: 256–262. https://doi.org/10.1016/j.eururo.2015.11.005.

[39] Sydes MR, Spears MR, Mason MD, Clarke NW, Dearnaley DP, de Bono JS, *et al*. Adding abiraterone or docetaxel to long-term hormone therapy for prostate cancer: directly randomised data from the STAMPEDE multi-arm, multi-stage platform protocol. Annals of Oncology. 2018; 29: 1235–1248. https://doi.org/10.1093/annonc/mdy072.

[40] Dai F, Chen Y, Huang L, Wang J, Zhang T, Li J, *et al*. A novel synthetic small molecule YH-306 suppresses colorectal tumour growth and metastasis via FAK pathway. Journal of Cellular and Molecular Medicine. 2015; 19: 383–395. https://doi.org/10.1111/jcmm.12450.

[41] Salberg UB, Skingen VE, Fjeldbo CS, Hompland T, Ragnum HB, Vlatkovic L, *et al*. A prognostic hypoxia gene signature with low heterogeneity within the dominant tumour lesion in prostate cancer patients. British Journal of Cancer. 2022; 127: 321–328. https://doi.org/10.1038/s41416-022-01782-x.

[42] Jayaprakash P, Ai M, Liu A, Budhani P, Bartkowiak T, Sheng J, *et al*. Targeted hypoxia reduction restores T cell infiltration and sensitizes prostate cancer to immunotherapy. The Journal of Clinical Investigation. 2018; 128: 5137–5149. https://doi.org/10.1172/JCI96268.

[43] Bery F, Figiel S, Kouba S, Fontaine D, Guéguinou M, Potier-Cartereau M, *et al*. Hypoxia Promotes Prostate Cancer Aggressiveness by Upregulating EMT-Activator Zeb1 and SK3 Channel Expression. International Journal of Molecular Sciences. 2020; 21: 4786. https://doi.org/10.3390/ijms21134786.

[44] Yang LH, Lee RKL, Kuo MH, Miao CC, Wang YX, Chen A, *et al*. Neuronal survival factor VGF promotes chemoresistance and predicts poor prognosis in lung cancers with neuroendocrine feature. International Journal of Cancer. 2022; 151: 1611–1625. https://doi.org/10.1002/ijc.34193.

[45] Yu L, Wei J, Liu P. Attacking the PI3K/Akt/mTOR signaling pathway for targeted therapeutic treatment in human cancer. Seminars in Cancer Biology. 2022; 85: 69–94. https://doi.org/10.1016/j.semcancer.2021.06.019.

[46] Ge X, Li M, Yin J, Shi Z, Fu Y, Zhao N, *et al*. Fumarate inhibits PTEN to promote tumorigenesis and therapeutic resistance of type2 papillary renal cell carcinoma. Molecular Cell. 2022; 82: 1249–1260.e7. https://doi.org/10.1016/j.molcel.2022.01.029.

[47] Cocco S, Leone A, Roca MS, Lombardi R, Piezzo M, Caputo R, *et al*. Inhibition of autophagy by chloroquine prevents resistance to PI3K/AKT inhibitors and potentiates their antitumor effect in combination with paclitaxel in triple negative breast cancer models. Journal of Translational Medicine. 2022; 20: 290. https://doi.org/10.1186/s12967-022-03462-z.

[48] Huang W, Xu Y. Analysis and Validation of Key Genes Related to Radiosensitivity in Prostate Cancer. Urology Journal. 2022; 20: 22–28. https://doi.org/10.22037/uj.v19i.6967.